

Journal Pre-proof

Nanomotion technology in combination with machine learning: a new approach for a rapid antibiotic susceptibility test for *Mycobacterium tuberculosis*

Anthony Vocat, Alexander Sturm, Grzegorz Jozwiak, Gino Cathomen, Michał Świątkowski, Roxana Buga, Grzegorz Wielgoszewski, Danuta Cichocka, Gilbert Greub, Onya Opota

PII: S1286-4579(23)00054-0

DOI: <https://doi.org/10.1016/j.micinf.2023.105151>

Reference: MICINF 105151

To appear in: *Microbes and Infection*

Received Date: 4 October 2022

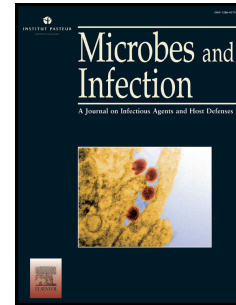
Revised Date: 10 May 2023

Accepted Date: 11 May 2023

Please cite this article as: A. Vocat, A. Sturm, G. Jozwiak, G. Cathomen, M. Świątkowski, R. Buga, G. Wielgoszewski, D. Cichocka, G. Greub, O. Opota, Nanomotion technology in combination with machine learning: a new approach for a rapid antibiotic susceptibility test for *Mycobacterium tuberculosis*, *Microbes and Infection*, <https://doi.org/10.1016/j.micinf.2023.105151>.

This is a PDF file of an article that has undergone enhancements after acceptance, such as the addition of a cover page and metadata, and formatting for readability, but it is not yet the definitive version of record. This version will undergo additional copyediting, typesetting and review before it is published in its final form, but we are providing this version to give early visibility of the article. Please note that, during the production process, errors may be discovered which could affect the content, and all legal disclaimers that apply to the journal pertain.

© 2023 Published by Elsevier Masson SAS on behalf of Institut Pasteur.



1 **Nanomotion technology in combination with machine learning: a**
2 **new approach for a rapid antibiotic susceptibility test for**
3 ***Mycobacterium tuberculosis***

4
5 Anthony Vocat^{a,b}, Alexander Sturm^b, Grzegorz Jozwiak^b, Gino Cathomen^b, Michał
6 Świątkowski^b, Roxana Buga^b, Grzegorz Wielgoszewski^b, Danuta Cichocka^b, Gilbert
7 Greub^{a,c}, Onya Opota^{a,*}.

8
9 ^{a)} Institute of Microbiology, Lausanne University Hospital and University of Lausanne,
10 Lausanne, 1011, Switzerland

11 ^{b)} Resistell AG, Muttens, 4132, Switzerland

12 ^{c)} Service of Infectious Diseases, Lausanne University Hospital and University of
13 Lausanne, Lausanne, 1011, Switzerland

14
15 *Corresponding author:

16 Institute of Microbiology, Lausanne University Hospital and University of Lausanne,
17 Rue du Bugnon 48, 1011 Lausanne, Switzerland.

18 Tel : +41 79 556 46 94, E-mail address : onya.opota@chuv.ch

19
20 **Abstract**

21 Nanomotion technology is a growth-independent approach that can be used to detect
22 and record the vibrations of bacteria attached to microcantilevers. We have developed
23 a nanomotion-based antibiotic susceptibility test (AST) protocol for *Mycobacterium*

24 *tuberculosis* (MTB). The protocol was used to predict strain phenotype towards
25 isoniazid (INH) and rifampicin (RIF) using a leave-one-out cross-validation (LOOCV)
26 and machine learning techniques.. This MTB-nanomotion protocol takes 21 hours,
27 including cell suspension preparation, optimized bacterial attachment to functionalized
28 cantilever, and nanomotion recording before and after antibiotic exposure. We applied
29 this protocol to MTB isolates (n=40) and were able to discriminate between susceptible
30 and resistant strains for INH and RIF with a maximum sensitivity of 97.4% and 100%,
31 respectively, and a maximum specificity of 100% for both antibiotics when considering
32 each nanomotion recording to be a distinct experiment. Grouping recordings as
33 triplicates based on source isolate improved sensitivity and specificity to 100% for both
34 antibiotics. Nanomotion technology can potentially reduce time-to-result significantly
35 compared to the days and weeks currently needed for current phenotypic ASTs for
36 MTB. It can further be extended to other anti-TB drugs to help guide more effective TB
37 treatment.

38

39 *Keywords:*

40 Antibiotic-susceptibility test

41 Atomic force microscopy

42 Nanomotion

43 Machine learning

44 Multi-drug resistant tuberculosis.

45 *Mycobacterium tuberculosis*

46 1. Introduction

47 Tuberculosis (TB) represents a major health concern. According to the World Health
48 Organization, there were more than 10 million new infections and 1.5 million deaths
49 caused by the bacterium in 2021. Furthermore, TB infection has become more difficult
50 to treat in recent decades due to the emergence of drug-resistant TB (DR-TB),
51 multidrug-resistant TB (MDR-TB), pre-extensively drug-resistant TB (pre-XDR-TB),
52 and extensively drug-resistant TB (XDR-TB), all of which are resistant to the core
53 currently employed antibiotics [1]. Effective TB treatment therefore requires (i) the use
54 of a combination of antibiotics to minimise the risk of resistance development and
55 emergence of MDR-TB, and (ii) a sufficient treatment duration to ensure cure
56 effectiveness and avoid relapse. Antibiotic susceptibility tests (ASTs) are used to
57 determine effective antibiotic combinations at start of treatment [2-5].

58 Currently, a combination of phenotypic and molecular methods are used to
59 assess *Mycobacterium tuberculosis* (MTB) antibiotic susceptibility. Culture-based
60 phenotypic assays are impaired by MTB's slow growth, meaning that data typically
61 only becomes available after patient treatment regimen decision-making and initiation
62 has already taken place [6, 7]. Molecular techniques for assessing drug susceptibility
63 and resistance such as polymerase chain reaction (PCR), probe hybridization assays,
64 or whole genome sequencing (WGS) offer a more rapid time-to-result [8-10]. However,
65 determining what targets to probe with genotypic AST assays depends on the
66 presence of previously characterised resistance mechanisms, which are not always
67 clearly defined for newer anti-TB drugs. These limitations call for new approaches for
68 the determination of antibiotic sensitivity for MTB.

69 Nanomotion-based AST is a novel approach using atomic force microscopy
70 (AFM) and nanomotion technology to detect and record nanoscale movements in

71 biological samples [11-14]. In AFM, nanomechanical sensors (micro-cantilevers)
72 oscillate when triggered by the organisms attached to their surface [15-17]. These
73 oscillations are detected by an optical readout system with a sensitivity of less than 0.1
74 Angstrom (0.01 nm) (Fig. 1a) [15, 11, 12, 14]. As such, nanomotion technology can be
75 adapted for bacterial phenotypic AST. Bacteria on the surface of a microcantilever will
76 generate cantilever deflections through their metabolic activity. Differences in
77 cantilever oscillations upon drug exposure depends on antibiotic susceptibility, hence
78 permitting the delineation of susceptible and resistant bacteria (Fig. 1) [15, 18].
79 Nanomotion-based AST requires small sample sizes (fewer than 1,000 bacteria), is
80 replication-independent, and can determine the presence of a resistance phenotype
81 within a few hours [15, 18]. It has already been successfully applied for various
82 bacterial strains, including *Staphylococcus aureus*, *Escherichia coli*, and *Bordetella*
83 *pertussis* [15, 18, 19].

84 MTB's cell wall and surface charge properties differ from previously studied
85 bacteria strains, thereby requiring a unique protocol for cantilever attachment. We
86 therefore aimed to develop and validate a rapid nanomotion-based AST method for
87 MTB that could overcome the limitations imposed by the strain's slow replication rate.
88 We herein present how nanomotion technology can drastically accelerate time-to-
89 result compared to existing phenotypic methods (Fig. 1b), representing a paradigm
90 shift in MTB phenotypic AST.

91 **2. Materials and methods**

92 *2.1. Bacterial strains, culture conditions, and antibiotic susceptibility tests*

93 *Mycobacterium bovis* BCG (ATCC[®] 35737), *M. smegmatis* mc²155 (ATCC[®] 700084),
94 and *M. tuberculosis* H37Rv (ATCC[®] 27294) strains were used to study mycobacteria

95 attachment to the cantilever. Clinical strains susceptible or resistant to isoniazid (INH)
96 and rifampicin (RIF) were obtained from the collection of the Institute of Microbiology
97 of Lausanne University Hospital. Bacteria were cultured in mycobacteria growth
98 indicator tubes (MGIT) incubated using an automated mycobacterial detection system
99 (BD BACTEC™ MGIT™). The MGIT method was also used to perform phenotypic AST
100 for first-line drugs. Molecular and phenotypic susceptibility testing for all strains was
101 conducted as previously described to determine susceptibility to INH and RIF [20, 21].
102 Bacterial minimal inhibitory concentrations (MICs) were determined using resazurin
103 microtiter plate assays (REMA). Molecular resistance to INH was determined by
104 analysing *inhA*, *katG*, and *oxyR* gene expression, as well as via WGS [21]. Molecular
105 resistance to RIF was determined by analysing *rpoB* gene expression [20, 22].

106

107 2.2. Reagents and antibiotics

108 Chitosan, dimethyl sulfoxide (DMSO), glutaraldehyde, phosphate buffered saline
109 (PBS), poly-diallyl-dimethylammonium chloride (pDADMAC), poly-D-lysine (PDL),
110 resazurin sodium salt, TWEEN 80, INH, and RIF were purchased from Sigma-Aldrich
111 (St. Louis, MO). MGITs and MGIT 960 supplement kits were purchased from Becton
112 Dickinson (Franklin Lakes, NJ). INH and other chemical agents were dissolved in
113 sterile water, while RIF was dissolved in DMSO.

114

115 2.3. Nanomotion-AST

116 To perform nanomotion-AST for MTB, we prepared MTB cell suspensions, attached
117 them to a functionalized cantilever, and recorded and analysed nanomotions in the
118 absence and presence of antibiotic agents. The overall protocol takes 21 hours, and
119 the full, detailed protocol can be found in the supplementary materials. We confirmed

120 efficient bacterial adhesion via two approaches: monitoring resonance frequency and
121 visual examination of bacterial presence on the cantilever before and after each
122 recording.

123

124 *2.4. Biosafety*

125 Initial validation was performed using *M. smegmatis*, *M. bovis* strain BCG, and *E. coli*
126 strains in BSL-1 and -2 laboratories. Subsequent validation using ATCC® and clinical
127 MTB strains were all performed in our BSL-3 laboratory. The nanomotion instrument
128 was placed under the laminar flow hood located in a BSL-3 environment, and was
129 connected to a computer using a cable (Fig. 2). All experiments were performed by
130 biologists or biomedical technicians with BSL-3 training and authorization to handle
131 MTB strains.

132 **3. Results**

133 *3.1. Microcantilever functionalization for M. tuberculosis attachment.*

134 Mycobacteria have waxy cell surfaces due to an abundance of mycolic acids and
135 various other lipids. Therefore, we tested a panel of functionalizing agents with different
136 chemical properties when examining MTB attachment to the cantilever. The cantilevers
137 were functionalized with either 20% (v/v) pDADMAC, 0.1 mg/mL PDL, 0.1 mg/mL
138 chitosan, or 0.5% (v/v) glutaraldehyde, after which *M. smegmatis*, *M. bovis* BCG, and
139 *M. tuberculosis* H37RV were sequentially applied. Immediately post-application,
140 bacteria were observed on the microcantilever for all four functionalizing agents.
141 However, after several washes with MGIT media, 20% (v/v) pDADMAC yielded the
142 best results. Although attachment with glutaraldehyde worked to some extent for *M.*
143 *smegmatis* and *M. bovis* BCG, it failed to maintain MTB attachment at the micro-

144 cantilever for which a superior attachment was obtained with pDADMAC 20% (Fig.
145 S2). We therefore decided to continue subsequent nanomotion experiments with 20%
146 (v/v) pDADMAC-functionalized micro-cantilevers.

147

148 *3.2. Development of a nanomotion-AST assay for M. tuberculosis.*

149 We developed a five-step workflow for nanomotion-based MTB AST (Fig. 1c).
150 Nanomotion technology is highly sensitive to external sources of vibrations, but
151 working with viable MTB strains requires a biosafety cabinet in a BSL-3 laboratory that
152 provides laminar air flow. We therefore had to use a noise isolation device to overcome
153 the vibrations emitted by the biosafety cabinet (Fig. 2), as well as test the reliability of
154 the instrument under laminar air flow. These tests were performed first using *E. coli* in
155 a BSL-1 laboratory before proceeding to MTB in a BSL-3 setting.

156 Each nanomotion recording began by reading the deflections generated by an
157 unloaded (bacteria-free) pDADMAC-functionalized cantilever for five minutes. This
158 was referred to as the blank portion of the recording, and is necessary to ensure
159 optimal sensor functionality and detect potential bacterial contamination within the
160 supplemented MGIT media in the measurement chamber. After this, the sensor would
161 be removed, loaded with bacteria, and returned to the measurement chamber.
162 Nanomotion recordings of the attached bacteria in supplemented MGIT were first
163 carried out for one hour in the absence of any antibiotic agent (the “bac” phase) in
164 order to capture baseline/endogenous oscillations. After this, INH or RIF was added
165 and bacterial oscillations were recorded for 20 hours (“drug” phase). The protocol
166 duration therefore totalled 21 hours.

167 Cantilever deflections were sampled at a frequency of 60 kHz. To visualize the
168 data, deflection variance for every ten seconds of recording was calculated during data

169 acquisition using a custom LabVIEW code (Fig. 3). However, raw data was used later
170 for classification model development. This workflow summarizes the first protocol for a
171 nanomotion-based AST for MTB under BSL-3 conditions.

172

173 *3.3. Prediction of isoniazid resistance using nanomotion-AST*

174 In order to use nanomotion technology for AST, there must be a set of parameters
175 within the nanomotion signal that can be used to discriminate between resistant and
176 susceptible strains. We therefore examined the clinical applicability of our AST protocol
177 by testing a set of forty sensitive and resistant clinical isolates from our MTB collection.

178 To examine whether our protocol could predict INH resistance, we examined 27
179 clinical isolates sensitive or resistant to INH. Each isolate was independently recorded
180 in triplicate (Table S1 and Fig. 3). Each recording within a triplicate was considered a
181 distinct experiment, which allowed us to compare separate recordings from the same
182 isolate and determine if experimental repetition would be needed for acceptable
183 performance. The same set-up was used for each isolate, while the raw data of
184 variance evolution throughout the experiments were visualised using a custom
185 LabVIEW code. In total, our INH dataset contained 39 recordings for INH-susceptible
186 strains and 38 recordings for INH-resistant strains, upon which we applied leave-one-
187 out cross validation (LOOCV).

188 Sensitivity assesses how well our method can predict a susceptible isolate, while
189 specificity assesses performance for prediction of resistance. A 100% performance
190 indicates no recordings falsely classified as a resistant strain. The correct identification
191 of a resistant strain is the most critical factor for avoiding the administration of an
192 ineffective antibiotic. Using seven free parameters, the algorithm was able to classify
193 the data with an accuracy of 96.1%, a sensitivity of 92.3% and a specificity of 100%.

194 With eight parameters, performance reached approximately greater-or-equal to 95%
195 for all three metrics (97.4% accuracy, 94.9% sensitivity and 100% specificity) (Fig. 3).

196 Similar performances were achieved when applying LOOCV at the sample level
197 — that is, each individual test set comprised all three triplicate recordings generated
198 from a given individual sample. Here, recording level performance was slightly lower
199 (seven parameters: 94.7% accuracy, 89.5% sensitivity, and 100% specificity; eight
200 parameters: 96.1% accuracy, 92.1% sensitivity, and 100% specificity) (Fig. 4).
201 However, we achieved the best performance by using LOOCV on single replicates and
202 subsequently combining the predictions for each triplicate using majority voting. Here,
203 a five parameter algorithm was sufficient to attain 100% accuracy, sensitivity, and
204 specificity (Fig. 4).

205

206 *3.4. Prediction of rifampicin resistance using nanomotion-AST*

207 We next applied the same approach to a dataset of 13 clinical isolates sensitive or
208 resistant to RIF with corresponding susceptible (n=18) or resistant (n=19) recordings.
209 A model based on a three-parameter algorithm was able to classify resistant and
210 susceptible strains using LOOCV at the recording level with a performance of 94.6%
211 accuracy, 94.4% sensitivity, and 94.7 % sensitivity. When the algorithm was extended
212 to include additional parameters (from four to twelve parameters), the dataset could be
213 perfectly delineated with 100% accuracy, 100% sensitivity, and 100 % specificity (Fig.
214 4). Applying LOOCV at the sample level (with triplicates grouped together) yielded a
215 performance of 97.2% accuracy, 94.4% sensitivity, and 100% specificity for four-
216 parameter algorithms and perfect delineation for five parameter algorithms (100%
217 accuracy, 100% sensitivity, and 100% specificity) (Fig. S7). When all three replicates

218 were utilised through the application of majority voting, both four- and five-parameter
219 algorithms exhibited 100 % accuracy, 100% sensitivity, and 100% specificity (Fig. S8).

220 4. Discussion

221 We have combined nanomotion technology and machine learning to develop a
222 novel rapid AST approach for MTB, and validated it for INH and RIF using a set of
223 clinical isolates with different minimum inhibitory concentrations (MICs). Though
224 nanomotion technology has been previously applied to investigate the impact of beta-
225 lactam antibiotics on various bacteria including *E. coli*, *B. pertussis*, and *S. aureus* [23,
226 24, 18, 19], this study is the first to establish a nanomotion-based AST that, in
227 combination with machine learning, can classify MTB isolates that are resistant or
228 susceptible to two major clinically-used antibiotics. A previous study on nanomotion
229 using the virulence-attenuated strain *M. bovis* BCG showed that mycobacterial viability
230 can be measured in response to antibiotic exposure [25]. However, this proof-of-
231 concept study did not aim to generally distinguish between sets of resistant and
232 susceptible strains [25].

233 By applying LOOCV, the models we built in the one-to-twelve-dimensional
234 parameter space were able to classify susceptible and resistant strains with high
235 confidence (over 95% accuracy, sensitivity, and specificity) for both INH and RIF. The
236 RIF model showed slightly better performance (incorporating fewer parameters). We
237 believe that this is because there is a greater gap between MICs of susceptible and
238 resistant isolates, as determined by resazurin microplate assay (REMA).

239 Nevertheless, prediction performance for both antibiotics could be improved by
240 applying majority voting to the three biological replicates and then combining sample-
241 level individual prediction outcomes, as well as finding parameters which can perfectly

242 delineate (100% accuracy) the data at the sample level. Therefore, a combination of
243 nanomotion recordings with advanced analyses by machine learning can be applied
244 as a highly sensitive and specific rapid AST for INH and RIF.

245 Working with MTB is very challenging since it possesses a slow growth rate and
246 work must be done under BSL-3 conditions. Nonetheless, we were able to include 40
247 clinical isolates in this study. Although limited, this number is still significant as the
248 isolates were not genetically related strains, but rather clinical isolates with different
249 genetic backgrounds. Since nanomotion-based AST performs well with antibiotics that
250 differ in their modes of action, this method can presumably be applied to other, more
251 recently-developed antibiotics such as bedaquiline, linezolid, and future drug
252 candidates [10, 21, 26].

253 Effective treatment of TB relies on drug regimen selection, which in turn
254 depends on reliable and timely access to AST data. As such, commonly used growth-
255 dependent assays underperform because of MTB's slow growth. Molecular and
256 genomic methods such as PCR and WGS are faster and show high performance for
257 some agents such as INH and RIF [27-29, 20], but are limited by high costs, little
258 applicability to novel drugs, and low flexibility. Nanomotion-based AST is a growth-
259 independent method, and thus circumvents the limitations of conventional phenotypic
260 ASTs, leading to a turnaround time of less than 24 hours.

261 There are several rapid antibiotic susceptibility tests available for more common
262 bacteria with known mechanisms of resistance. Enzymatic tests, for instance, can be
263 used to detect the degradation of agents such as β -lactamase or carbapenemase.
264 These tests are also helpful for predicting resistance to specific antibiotics. Indeed,
265 new molecular-based rapid antibiotic tests for TB such as the Xpert MTB/RIF test allow
266 for the rapid prediction of resistance to rifampicin [30]. However, there are currently no

267 rapid phenotypic tests available for TB that can be used for either new drugs or drugs
268 with poorly understood resistance mechanisms. Since phenotypic tests are particularly
269 useful when the mechanism of resistance is unknown, there is a need for the
270 development of new, rapid phenotypic tests that can be used to diagnose and treat TB
271 more effectively.

272 Another advantage of nanomotion-based AST is that it requires a specimen size
273 of only approximately 100 bacteria [19, 17]. This allows the possibility of testing several
274 antibiotics in parallel using the same positive culture, as well as testing antibiotic
275 combinations. In our previous study on bacteremia, we combined nanomotion
276 technology with a simple method for purifying and concentrating bacteria from positive
277 blood cultures in order to develop a rapid AST against bloodstream infection agents
278 [19]. In the long run, nanomotion technology applied to tuberculosis may reduce MGIT
279 culture incubation times, or even permit AST to begin directly with purified bacteria
280 obtained from a clinical sample such as bronchial aspirate sputum or bronchoalveolar
281 lavage. It is important to ensure that bacteria remain on the cantilever throughout the
282 experiment to avoid signal variation resulting from bacterial loss instead of response
283 to antibiotic treatment. To ensure efficient bacterial adhesion, we validated the efficacy
284 of pDADMAC as a linking agent and visually checked for the presence of bacteria on
285 the cantilever before and after all recordings. Additionally, we monitored resonance
286 frequency variations to confirm bacterial attachment to the cantilever — namely,
287 resonance frequency should not vary if bacterial attachment remains unchanged
288 during experimentation. Furthermore, the method is species agnostic, which makes it
289 an interesting tool for non-TB mycobacteria, such as *M. abscessus*, that also often
290 presents multi-resistance phenotypes [31].

291 Nanomotion represents a new paradigm for predicting antibiotic
292 susceptibility/resistance [32]. The antibiotic concentrations used for nanomotion AST
293 do not correspond to the critical concentrations of antibiotics as defined by the
294 EUCAST or recommended by the WHO when currently performing classical AST [6,
295 7]. Due to the very limited antibiotic exposure time (under 24 hours in this study),
296 nanomotion AST may not be fully suitable for MIC determination, even though it can
297 discriminate between sensitive and resistant organisms. Whether nanomotion can
298 distinguish metabolic variations or stress responses is something that would be
299 interesting to explore in future studies. Indeed, bacterial metabolism state (growing
300 versus latent) has been associated with resistance and tolerance mechanisms in MTB
301 [33, 34]. Nanomotion technology enables us to measure bacterial response to
302 antibiotic exposure without relying on bacterial growth-dependent metrics such as MIC
303 or minimum bactericidal concentration (MBC). That said, a correlation has been
304 demonstrated between MIC values and nanomotion signals [15]. As for MBC, it is
305 important to note that 22 hours of incubation may not be sufficient to kill all bacteria
306 [35]. The changes in nanomotion signal observed in this study may be attributed to
307 metabolic changes, something that warrants further investigation in future studies.
308 Further, this technology holds great potential for antibiotic susceptibility testing as it
309 allows for direct measurement of bacterial response to antibiotics without the need for
310 sub-culturing. As such, using nanomotion to test the impact of different antibiotic
311 concentrations may provide new and complementary information on MTB resistance
312 or tolerance to anti-tuberculosis agents. It will be important for the nanomotion
313 technology to be available in multi-channels in the future, to allow for an efficient use
314 in clinical settings or drug discovery. This will increase throughput and enable testing
315 of multiple antibiotics in parallel. The ability to test multiple antibiotics in parallel using

316 multi-channel technology would greatly improve the speed and efficiency of antibiotic
317 susceptibility testing, particularly in the context of drug discovery where large numbers
318 of compounds need to be screened for potential antimicrobial activity. Furthermore,
319 multi-channel technology could facilitate the testing of antibiotic combinations, which
320 are essential for the treatment of both susceptible tuberculosis and MDR-XDR
321 tuberculosis.

322 This study presents an innovative growth-independent AST method applicable
323 to BSL-3 conditions, developed first for fast-growing bacteria and then adapted and
324 validated for MTB. This method needs to be further examined in a larger study, as well
325 as tested against low-level and heterogeneous resistant strains to support further
326 development as an in vitro diagnostic test. This approach also represents a new tool
327 for the study of growth-independent drug responses. Our results open the door for
328 further method development and pre-clinical studies using nanomotion technology to
329 examine MTB isolates, working towards the ultimate goal of developing an AST
330 possessing high performance and short time-to-result, thereby combining the
331 advantages of broadly applicable phenotypic ASTs and rapid molecular diagnostic
332 methods.

333

334 **Declaration of competing interest**

335 This work was supported by Innosuisse - Swiss Innovation Agency through 36334.1
336 IP-LS grant to Prof. G. Greub representing the academic partner (Institute of
337 Microbiology of the University of Lausanne) and Dr D. Cichocka representing the
338 company (Resistell AG).

339 Dr D. Cichocka is the CEO of Resistell and R. Buga, G. Cathomen, G. Jozwiak, A.
340 Sturm, M. Swiatkowski, G. Wielgoszewski are all employed by Resistell AG. A. Vocat
341 is employed by both Institute of Microbiology of the University of Lausanne and

342 Resistell AG. Prof. Gilbert Greub is a medical advisor for Resistell AG. Dr Onya Opota
343 was responsible for the part of the InnoSuisse project dedicated to Mycobacteria.

344

345 **Acknowledgments**

346 This work was supported by Innosuisse - Swiss Innovation Agency through 36334.1
347 IP-LS grant to Prof. G. Greub and Dr. D. Cichocka. The authors thank the biomedical
348 technicians specialising in mycobacteria: G. Gonzalez, M. Kilchoer, J. Ducrot, and V.
349 Martin for technical assistance. We also thank Prof. S.T. Cole for sharing *M.*
350 *tuberculosis* reference strains with us, as well as Prof. J. McKinney and Dr. N. Dhar for
351 *M. smegmatis* strains. Finally, we thank M. Luczynska for help with figure design.

352

353 Appendix A. Supplementary data

354 References

- 355 [1] Murray CJL, Ikuta KS, Sharara F, Swetschinski L, Robles Aguilar G, Gray A, et al. Global burden of
356 bacterial antimicrobial resistance in 2019: a systematic analysis. *The Lancet* 2022;399:629-55.
- 357 [2] Antimycobacterial Susceptibility Testing G, Georghiou SB, Rodwell TC, Korobitsyn A, Abbadi SH,
358 Ajbani K, et al. Updating the approaches to define susceptibility and resistance to anti-tuberculosis
359 agents: implications for diagnosis and treatment. *European Respiratory Journal* 2022;59:2200166.
- 360 [3] Aghayee S, Benadiba C, Notz J, Kasas S, Dietler G, Longo G. Combination of fluorescence
361 microscopy and nanomotion detection to characterize bacteria. *J Mol Recognt* 2013;26:590-5.
- 362 [4] Acquah R, Furin J. Universal regimens or universal access to drug susceptibility testing for
363 tuberculosis? *The Lancet Infectious Diseases* 2019;19:224-5.
- 364 [5] Antimycobacterial Susceptibility Testing G. Updating the approaches to define susceptibility and
365 resistance to anti-tuberculosis agents: implications for diagnosis and treatment. *The European*
366 *respiratory journal* 2022;59:2200166.
- 367 [6] Schön T, Werngren J, Machado D, Borroni E, Wijkander M, Lina G, et al. Antimicrobial susceptibility
368 testing of *Mycobacterium tuberculosis* complex isolates - the EUCAST broth microdilution reference
369 method for MIC determination. *Clinical microbiology and infection : the official publication of the*
370 *European Society of Clinical Microbiology and Infectious Diseases* 2020;26:1488-92.
- 371 [7] Schön T, Werngren J, Machado D, Borroni E, Wijkander M, Lina G, et al. Multicentre testing of the
372 EUCAST broth microdilution reference method for MIC determination on *Mycobacterium*
373 *tuberculosis*. *Clinical Microbiology and Infection* 2021;27:288.e1-e4.
- 374 [8] Walker TM, Kohl TA, Omar SV, Hedge J, Del Ojo Elias C, Bradley P, et al. Whole-genome
375 sequencing for prediction of *Mycobacterium tuberculosis* drug susceptibility and resistance: a
376 retrospective cohort study. *The Lancet. Infectious diseases* 2015;15:1193-202.
- 377 [9] Walker TM, Merker M, Kohl TA, Crook DW, Niemann S, Peto TE. Whole genome sequencing for
378 M/XDR tuberculosis surveillance and for resistance testing. *Clinical microbiology and infection : the*
379 *official publication of the European Society of Clinical Microbiology and Infectious Diseases*
380 2017;23:161-6.
- 381 [10] Walker TM, Miotto P, Köser CU, Fowler PW, Knaggs J, Iqbal Z, et al. The 2021 WHO catalogue of
382 *Mycobacterium tuberculosis* complex mutations associated with drug resistance: a genotypic analysis.
383 *The Lancet Microbe* 2022;3:e265-e73.
- 384 [11] Alonso-Sarduy L, De Los Rios P, Benedetti F, Vobornik D, Dietler G, Kasas S, et al. Real-time
385 monitoring of protein conformational changes using a nano-mechanical sensor. *PloS one*
386 2014;9:e103674.
- 387 [12] Kasas S, Ruggeri FS, Benadiba C, Maillard C, Stupar P, Tournu H, et al. Detecting nanoscale
388 vibrations as signature of life. *Proc Natl Acad Sci U S A* 2015;112:378-81.
- 389 [13] Kasas S, Stupar P, Longo G, Dietler G. [Detecting life thanks to the atomic force microscope]. *Med*
390 *Sci (Paris)* 2015;31:369-71.

- 391 [14] Kasas S, Stupar P, Dietler G. AFM contribution to unveil pro- and eukaryotic cell mechanical
392 properties. *Semin Cell Dev Biol* 2018;73:177-87.
- 393 [15] Longo G, Alonso-Sarduy L, Rio LM, Bizzini A, Trampuz A, Notz J, et al. Rapid detection of bacterial
394 resistance to antibiotics using AFM cantilevers as nanomechanical sensors. *Nat Nanotechnol*
395 2013;8:522-6.
- 396 [16] Ghaemi N, Nikoobin A, Ashory MR. A Comprehensive Categorization of Micro/Nanomechanical
397 Resonators and Their Practical Applications from an Engineering Perspective: A Review. *Advanced*
398 *Electronic Materials* 2022;n/a:2200229.
- 399 [17] Al-madani H, Du H, Yao J, Peng H, Yao C, Jiang B, et al. Living Sample Viability Measurement
400 Methods from Traditional Assays to Nanomotion. *Biosensors* 2022;12:453.
- 401 [18] Kasas S, Malovichko A, Villalba MI, Vela ME, Yantorno O, Willaert RG. Nanomotion Detection-
402 Based Rapid Antibiotic Susceptibility Testing. *Antibiotics* 2021;10:287.
- 403 [19] Stupar P, Opota O, Longo G, Prod'hom G, Dietler G, Greub G, et al. Nanomechanical sensor
404 applied to blood culture pellets: a fast approach to determine the antibiotic susceptibility against agents
405 of bloodstream infections. *Clinical microbiology and infection : the official publication of the European*
406 *Society of Clinical Microbiology and Infectious Diseases* 2017;23:400-5.
- 407 [20] Opota O, Senn L, Prod'hom G, Mazza-Stalder J, Tissot F, Greub G, et al. Added value of molecular
408 assay Xpert MTB/RIF compared to sputum smear microscopy to assess the risk of tuberculosis
409 transmission in a low-prevalence country. *Clinical microbiology and infection : the official publication of*
410 *the European Society of Clinical Microbiology and Infectious Diseases* 2016;22:613-9.
- 411 [21] Laurent S, Zakham F, Bertelli C, Merz L, Nicod L, Mazza-Stalder J, et al. Genome sequencing of
412 *Mycobacterium tuberculosis* clinical isolates revealed isoniazid resistance mechanisms undetected by
413 conventional molecular methods. *Int J Antimicrob Agents* 2020;56:106068.
- 414 [22] Opota O, Zakham F, Mazza-Stalder J, Nicod L, Greub G, Jatton K. Added Value of Xpert MTB/RIF
415 Ultra for Diagnosis of Pulmonary Tuberculosis in a Low-Prevalence Setting. *Journal of clinical*
416 *microbiology* 2019;57.
- 417 [23] Arnal L, Longo G, Stupar P, Castez MF, Cattelan N, Salvarezza RC, et al. Localization of adhesins
418 on the surface of a pathogenic bacterial envelope through atomic force microscopy. *Nanoscale*
419 2015;7:17563-72.
- 420 [24] Villalba MI, Stupar P, Chomicki W, Bertacchi M, Dietler G, Arnal L, et al. Nanomotion Detection
421 Method for Testing Antibiotic Resistance and Susceptibility of Slow-Growing Bacteria. *Small* 2018;14.
- 422 [25] Mustazzolu A, Venturelli L, Dinarelli S, Brown K, Floto RA, Dietler G, et al. A Rapid Unraveling of
423 the Activity and Antibiotic Susceptibility of *Mycobacteria*. *Antimicrobial agents and chemotherapy*
424 2019;63.
- 425 [26] Kadura S, King N, Nakhoul M, Zhu H, Theron G, Köser CU, et al. Systematic review of mutations
426 associated with resistance to the new and repurposed *Mycobacterium tuberculosis* drugs bedaquiline,
427 clofazimine, linezolid, delamanid and pretomanid. *J Antimicrob Chemother* 2020;75:2031-43.
- 428 [27] Wang L, Yang J, Chen L, Wang W, Yu F, Xiong H. Whole-genome sequencing of *Mycobacterium*
429 *tuberculosis* for prediction of drug resistance. *Epidemiol Infect* 2022;150:e22.

- 430 [28] Consortium CR, the GP, Allix-Beguec C, Arandjelovic I, Bi L, Beckert P, et al. Prediction of
431 Susceptibility to First-Line Tuberculosis Drugs by DNA Sequencing. *The New England journal of*
432 *medicine* 2018;379:1403-15.
- 433 [29] Boehme CC, Nabeta P, Hillemann D, Nicol MP, Shenai S, Krapp F, et al. Rapid molecular detection
434 of tuberculosis and rifampin resistance. *The New England journal of medicine* 2010;363:1005-15.
- 435 [30] Chakravorty S, Simmons AM, Rowneki M, Parmar H, Cao Y, Ryan J, et al. The New Xpert MTB/RIF
436 Ultra: Improving Detection of *Mycobacterium tuberculosis* and Resistance to Rifampin in an Assay
437 Suitable for Point-of-Care Testing. *MBio* 2017;8.
- 438 [31] Daley CL, Iaccarino JM, Lange C, Cambau E, Wallace RJ, Jr., Andrejak C, et al. Treatment of
439 Nontuberculous Mycobacterial Pulmonary Disease: An Official ATS/ERS/ESCMID/IDSA Clinical
440 Practice Guideline. *Clinical Infectious Diseases* 2020;71:905-13.
- 441 [32] Stojanovic Z, Gonçalves-Carvalho F, Marín A, Abad Capa J, Domínguez J, Latorre I, et al. Advances
442 in diagnostic tools for respiratory tract infections. From tuberculosis to COVID19: changing paradigms?
443 *ERJ Open Research* 2022;00113-2022.
- 444 [33] Smith T, Wolff KA, Nguyen L. Molecular biology of drug resistance in *Mycobacterium tuberculosis*.
445 *Curr Top Microbiol Immunol* 2013;374:53-80.
- 446 [34] de Steenwinkel JE, de Knecht GJ, ten Kate MT, van Belkum A, Verbrugh HA, Kremer K, et al. Time-
447 kill kinetics of anti-tuberculosis drugs, and emergence of resistance, in relation to metabolic activity of
448 *Mycobacterium tuberculosis*. *J Antimicrob Chemother* 2010;65:2582-9.
- 449 [35] de Steenwinkel JEM, de Knecht GJ, ten Kate MT, van Belkum A, Verbrugh HA, Kremer K, et al.
450 Time-kill kinetics of anti-tuberculosis drugs, and emergence of resistance, in relation to metabolic
451 activity of *Mycobacterium tuberculosis*. *Journal of Antimicrobial Chemotherapy* 2010;65:2582-9.
- 452
- 453

454 **Tables and figures**

455 **Figure Legends**

456 **Figure 1. Principles of a nanomotion-based *M. tuberculosis* AST approach.** (A) A
457 laser is emitted on a microcantilever nanomotion sensor and reflected on a position-
458 sensitive photodetector that records its deflection (*Stupar, Opota et al. 2017 Clin*
459 *Microbiol Infect*). Environmental background noise generates a very low level of
460 vibrations detected on an empty microcantilever, and this is used as the blank control.
461 Live bacteria attached to the microcantilever make nanoscale movements
462 (nanomotion). These vibrations lead to an increased deflection of the microcantilever.
463 Upon exposure to an inhibiting compound such as an effective anti-TB agent, bacterial
464 vibrations from the attached TB strain decrease. The degree of the microcantilever
465 deflection is recorded as the variance. (B) Comparison of nanomotion-based AST and
466 conventional phenotypic AST for tuberculosis. (C) Experimental procedure and
467 preparation of nanomotion AST: i) centrifugation of a positive mycobacteria growth
468 indicator tube (MGIT), ii) resuspension of the bacterial pellet in fresh MGIT medium, iii)
469 MTB strains are attached to functionalized cantilevers by immersing the cantilever in a
470 bacterial suspension for 5 minutes, iv) transfer of the cantilever with attached cells to
471 the nanomotion recording chamber for recording or v) recording and analysis.

472

473

474 **Figure 2. Configuration of nanomotion instrument under biosafety cabinet in a**
475 **biosafety laboratory level 3. Lower panel:** (a) Biosafety cabinet located in a BSL-3
476 laboratory (b) nanomotion device; (c) compact laser module, (d) low-profile
477 nanomotion device for easy operation in biosafety cabinet, (e) operator with personal

478 protective equipment for BSL-3 laboratory , (f) optical microscope with integrated
479 screen, (g) laptop with LabVIEW control software. **Upper left panel:** (h) optical
480 microscope with integrated screen. **Upper right panel:** nanomotion instrument (i)
481 measurement head, (j) protective lid, (k) laser plug, (l) vibration damping unit, (m)
482 control and acquisition unit.

483

484

485 **Figure 3. *Mycobacterium tuberculosis* cantilever attachment and subsequent**
486 **nanomotion variance recordings.** Microcantilevers from NANOSENSORS™ have
487 the following dimensions: length 120-130 μm , width 33-37 μm , thickness 720-780 nm.
488 Microcantilevers were washed four times with PBS and then incubated with MTB for 5
489 minutes. Mycobacteria attachment quality was evaluated by microscopy. Images were
490 taken using an EVOS™ XL Core Imaging System (A) before the start of and (B) after
491 the end of nanomotion recording experiments. The pre-experiment image served as
492 the attachment control and showed typical MTB "cords", while the post-experiment
493 image confirmed the absence of any significant detachment or attachment of bacteria
494 on the microcantilever. MTB linical strains obtained from our diagnostic laboratory were
495 selected based on their susceptibility or resistance to isoniazid (INH) or rifampicin
496 (RIF). Upon MTB attachment to the cantilever, we observed a significantly higher
497 nanomotion variance compared to the blank phase. After the addition of INH, both
498 susceptible (C) and resistant (D) strains responded, although they responded
499 differently. Towards the end of the experiment, bacterial vibrational variance was
500 greater in resistant strains than susceptible strains. (E) and (F) MIC distribution for INH
501 (E) and RIF (F) of the MTB strain genotypes used for this validation study.

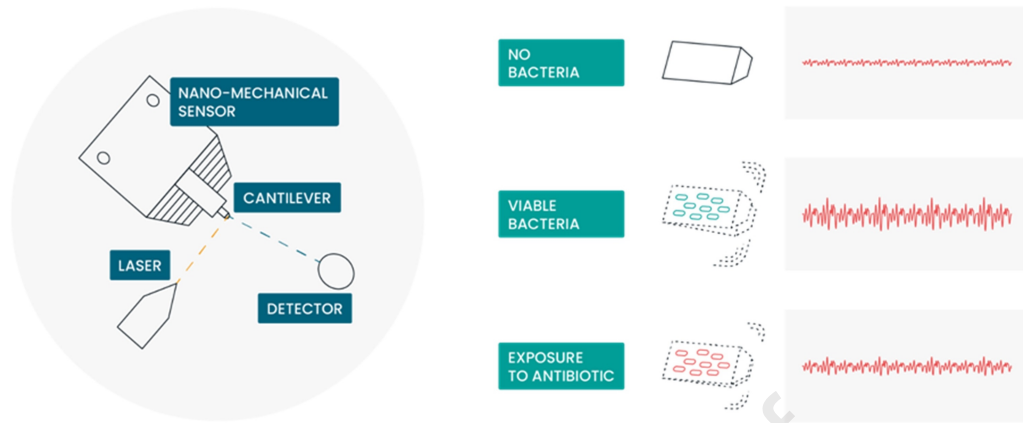
502

503

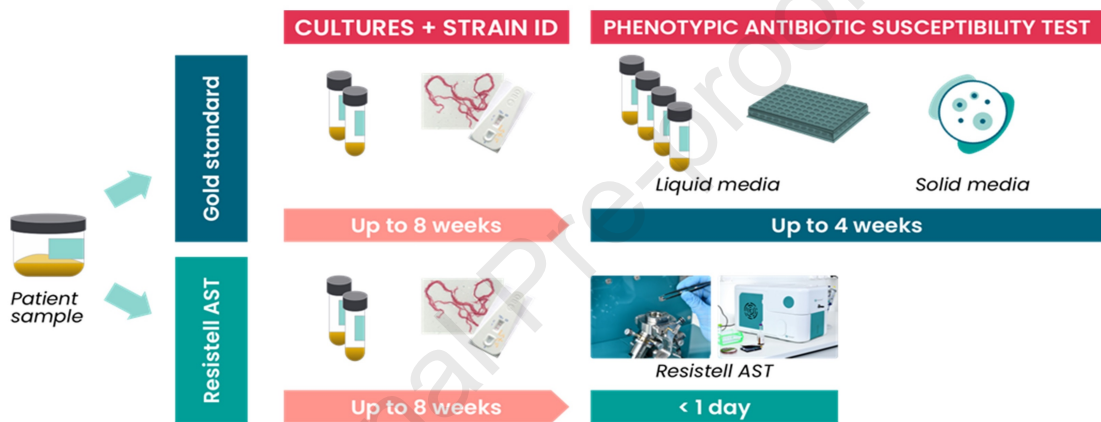
504 **Figure 4. Classification performance evaluated with LOOCV at the recording**
505 **level for the isoniazid dataset.** Algorithm complexity increased from a single
506 parameter up to 12 parameters (separation in 1-12 dimensional feature space).

Journal Pre-proof

A



B



C

